Electrowetting-driven Solar Trackers (EST) for Concentrated Photovoltaic (CPV) Rooftop Applications

Sung-Yong Park, Jennifer Kuo, and Kyle Gould

Teledyne Scientific & Imaging, Thousand Oaks, CA, 91360 USA
E-mail: spark@teledyne-si.com

ABSTRACT

Concentrated photovoltaics (CPV) is an alternative solution to save the material cost of solar photovoltaic (PV) systems. However, CPV requires an expensive, complex, bulky, and heavy solar tracker that allows following sun's position. These bulky and heavy mechanical trackers significantly increase the installation cost of the CPV systems as well as require high power consumption for the operation. These issues make CPV systems difficult to be used on a residential rooftop. In this paper, we present an electrowetting-driven solar tracker (EST) for a CPV rooftop application. Solar tracking principle of the EST is based on an electrowetting effect which does not require any mechanical tracking components. By eliminating such bulky and heavy mechanical solar tracking parts, total cost and power consumption of the CPV system are dramatically reduced, resulting in a high-efficiency concentrated solar power system on a rooftop.

Keywords: solar trackers, concentrated photovoltaic (CPV), solar photovoltaic (PV), electrowetting, optofluidics

1 INTRODUCTION

Solar PV systems have attracted as promising clean energy alternatives to traditional electricity generation sources, such as coal or natural gas-burning power plants. One biggest obstacle to the widespread deployment of PV systems is that they are not cost competitive with traditional sources [1, 2]. A CPV technology, which uses additional optics to concentrate a large amount of sunlight onto a small cell, could be a solution to reduce the PV cost. One key component of the CPV is a solar tracker that enables to orient the optics toward sun's position. However, current CPV solar trackers are very expensive, complex, bulky, and heavy (loaded weight about ~3000kg for dual-axis trackers), because they consist of many mechanical moving parts such as motors and supporting frames [3]. Not only do such complex and heavy mechanical trackers increase the CPV installation cost, but also require high power consumption for operation. These issues greatly prevent CPV from being installed on for a residential rooftop.

In this paper, we report an electrowetting-driven solar tracker (EST) for a CPV rooftop application. The EST system consists of an array of tunable liquid prisms. An apex angle of each prism is actively controlled by electrowetting, enabling to re-direct incident sunlight for solar concentration without any bulky and heavy mechanical solar trackers. Our EST can provide several unique advantages over conventional mechanical trackers, including (1) low power consumption in the range of ~mW; (2) low cost and simple supporting hardware that can save space and weight of the trackers; (3) adaptive solar tracking without any mechanical moving parts; and (4) quiet operation for a residential rooftop application.

2 THEORY

Electrowetting is one of the promising approaches that can effectively handle micro/meso-scale liquid droplets. Its advantages include, extremely low power consumption, rapid response time, no mechanical pump for fluidic transport and easy implementation. Due to these unique characteristics, it has been used for wide applications such as lab-on-a-chip [4, 5], on-chip cooling [6-8], electronic paper [9], and tunable optical lens [10].

An elecrowetting principle can be explained by a Young-Lippmann equation [11], describing that the contact angle of a droplet sitting on a solid surface can be dominantly controlled by the electric voltage drop across a dielectric layer:

$$\cos\theta = \cos\theta_0 + \frac{1}{2\gamma}cV^2 \qquad (1)$$

where c is the specific capacitance, t is thickness of the dielectric layer, γ is the surface tension between two immiscible fluids, θ_0 and θ represent the contact angles before and after an external voltage application. In EST, the contact angle (θ) is the angle of an aqueous droplet on the sidewall surface.

3 DEVICE STRUCTURE AND WORKING PRINCIPLE

A schematic of the EST device and its working principle are illustrated in Figure 1. The sidewall of a single liquid prism module consists of a hydrophobic and dielectric layer deposited on a ITO substrate: 120 nm thick aluminum oxide
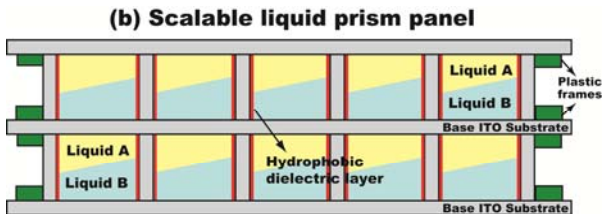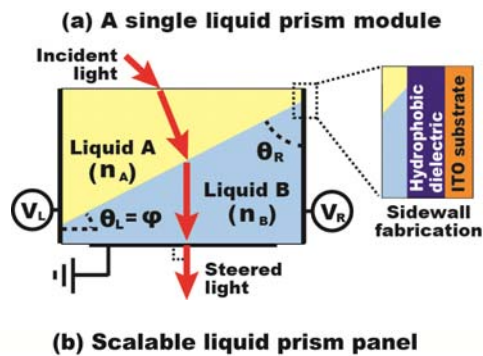
(a) A single liquid prism module

(b) Scalable liquid prism panel

Figure 1. A schematic of the EST device structure and its working principle. (a) A single liquid prism module consists of two immiscible liquids in a transparent cuvette. The cuvette sidewall is fabricated by coating a hydrophobic dielectric layers on a ITO substrate. An elecrtowetting effect is induced by an applied bias voltage and determines an apex angle, φ, of the liquid prism. Then an incident light is steered due to the refractive index difference between two liquids. (b) By stacking up and expanding a prism module, a large-scale liquid prism panel is achieved.

(Al_2O_3) and 50 nm thick hydrophobic (FluoroPel PFC 1601V, Cytonix) layers. A UV curable epoxy (Norland) was used to assemble the four sidewalls on the base ITO substrate and form a transparent cuvette. Two immiscible liquids (e.g. water and oil) are filled in the cuvette and then covered by a top transpent plate. The refractive indices of two liquids are denoted by n_A and n_B, respectively. The fluid-fluid interface naturally forms a curved-shaped meniscus in the cuvette due to the Laplace pressure. We apply bias voltages of V_L in the left and V_R in the right sidewalls and the base ITO substrate is grounded. An electrowetting effect controls the contact angles (θ_L and θ_R) of an aqueous droplet at each sidewall. As a result, the fluid-fluid interface keeps straight and its orientation determines an apex angle (φ), functioning as a tunable optical prism. Incident light can then be steered by using two immiscible liquids with high refractive index difference. An applied electric input varies in each of the sidewalls to continuously tune the apex angle of the liquid prism. Incident sunlight is then adaptively steered for daily and seasonal solar tracking without any mechanical moving parts. To increase an aperture area and a light refraction capability, a single liquid prism module is further stacked up and expanded to achieve a large-scale liquid prism panel. Figure 1(b) shows an example of the stacked dual prism.
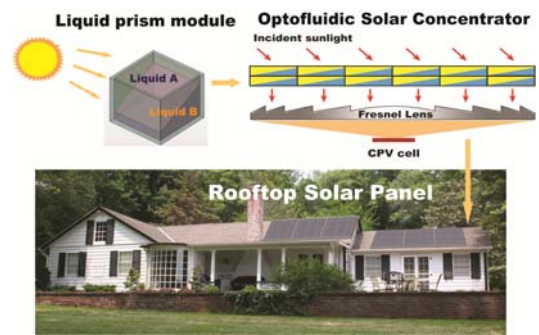

Figure 2. An electrowetting-driven solar tracking (EST) system for CPV rooftop application. A single liquid prism is further stacked up and expanded to achieve a large-scale liquid prism panel. The integration with a Fresnel lens allows CPV technologies to be used for a residential rooftop application.

Figure 2 shows an electrowetting-driven solar tracking (EST) system installed for a CPV rooftop application. Incoming sunlight is assumed to be collimated beam. The EST system adaptively steers and re-direct it toward a Fresnel lens that is placed underneath the liquid prism panel. Then the sunlight is concentrated onto the small CPV cell. The integration with a Fresnel lens significantly increases an area reduction ratio. Unlike conventional CPV solar trackers, our EST system does not require any bulky and heavy mechanical moving components such as motors and supporting frames.

4 OPTICAL LIQUID MATERIALS AND PERFORMACE ANALYSIS

For the best performance of our solar liquid prism, optical liquid materials have to be carefully selected. There are several critical conditions that the liquid materials need to satisfy. First the refractive index contrast between two immiscible liquids shold be large to increase a prism refraction capability. Second they should be optically clear to minimize solar energy loss. Third both liquid materials have wide temperature range that they can stand without freezing and volatility. The last key condition is that the liquids should well response with an electrowetting effect. This would include the material properties such as surface tension, viscosity, density, and so on.

We have further carried out an optical analysis of liquid prism to predict the performance and develop our solar tracking algorithm. The optical path of a single liquid prism is illustrated in Figure 3. The refractive indices are n_{air} for air, n_A for Liquid A, and n_B for Liquid B, respectively. The angles of incident and refracted light at each interface are denoted by α and β, and their subscripts of A and B indicate the Liquid A and B. An apex angle of the prism is denoted by φ, which is controlled by an electrowetting effect. Since
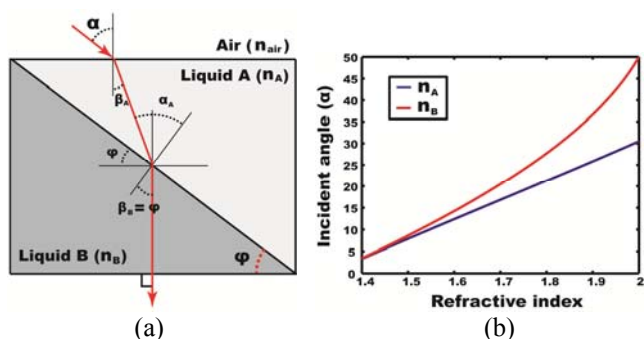
(a)   (b)

Figure 3. (a) An optical path is created in a single liquid prism composed of Liquid A and Liquid B. (b) Optical analysis is conducted to predict the solar tracking angle that can adjusted by the liquid prism. The apex angle of the prism that is controlled by electrowetting is assumed to be 40°. The blue line indicates the incident angle (α) as increasing n_A, when n_B is fixed as 1.33. Reversely, the red line represents α with the increase of n_B, while n_A is fixed as 1.33. Solar tracking range (α) is considerably enhanced by the increase of n_B, the refractive index of Liquid B located in the lower side of the prism.

the angle of the final outgoing light must be perpendicular to the bottom prism surface for the high concentration of sunlight, the angle of β_B is equal to the apex angle, φ, by the geometry. We apply the Snell's law at each of the interfaces and obtain the incident angle (α) that can be re-directed by our liquid prism. The angle (α) is expressed as:

$$\alpha = \sin^{-1}\left(n_B \sin\varphi \cos\varphi - n_A \sin\varphi \sqrt{1 - \left(\frac{n_B}{n_A}\sin\varphi\right)^2} \right) \quad (2)$$

which is a function of the refractive indices and the prism apex angle. This equation provides us valuable information on solar tracking algorithm how large the prism apex angle (φ) is required. In other words, it tells us how much bias voltage is required to tilt the fluid-fluid interface.

Figure 3(b) shows the prism performance regarding the tracking angle (α) that the liquid prism can adjust. First we assume that $n_B = 1.33$ and an apex angle (φ) controlled by elecrowetting is 40°. The result is represented by a blue line. Incident sunlight angle almost linearly rises up with the increase of n_B from 1.4 to 2.0. The next calculation assumes that n_A is fixed as 1.33 and n_B increase from 1.4 to 2.0. The range (α) of incident sunlight that can be adjusted by the liquid prism is dramatically enhanced up to ±50° (see a red line). From these analytical results, one can know that the increase of n_B, the refractive index of Liquid B located in the lower side of the prism, has effectively influence on the tracking range.

Figure 4(a) shows an optical path in the dual prism achieved by overlapping two liquid prisms. We assume that the prism consists of water (n_{water}=1.33) and commercially-available optical oil, SL-5267 from SantoLight that has the
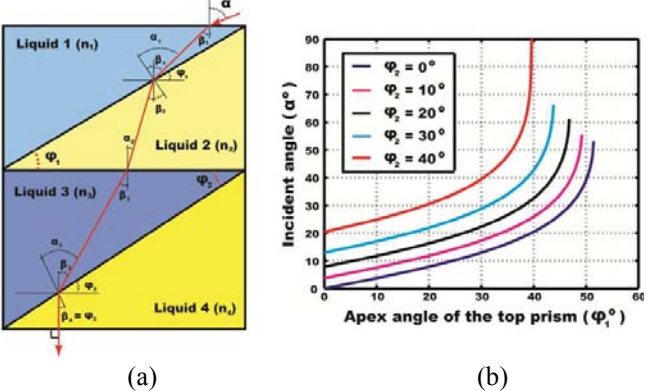

(a)   (b)

Figure 4. (a) An optical path is created in a dual prism. It is fabricated by stacking two single liquid prisms and thus Liquid 1 and 3 is the same material, and Liquid 2 and 4 as well. (b) Performance of the dual prism is predicted. When the apex angles in the top and bottom prisms is controlled to φ_1= 40° and φ_2=40°, the dual prism can achieve wide tracking angle up to α=±70° without any bulky and heavy mechanical moving parts.

refractive index as high as 1.67. The dual prism is estimated to steer the incident sunlight with the tracking angle up to α=±70° at φ_1= 40° and φ_2=40°.

5 EXPERIMENTAL RESULTS

For the experiments, the cuvette was fabricated with the size of $1.0 \times 1.0 \times 2.0$ cm^3 and filled with de-ionized (DI) water and silicone oil (Dow Corning). Because of the slight density difference between two liquids, water is located in the lower side. For the interface stability, we added 1 wt % of sodium dodecyl sulfate (SDS) surfactant into DI water and its surface tension was lowered from 73 mN/m to 8.6 mN/m. Surfactant is also preferable to reduce the bias voltage required for a given contact angle change. According to Eq. (1), the contact angle change is inversely proportional to the surface tension (γ) of an aqueous droplet. An electronic controller was designed to generate sqaure-wave ac voltage at low frequncy. This is because a long period application with a dc bias may cause irreversible polarization, resulting in damage on the dielectric layer.

Figure 4 shows photographs of an electrowetting-driven liquid prism modulation. Before an ac bias voltage is applied to the prism, the fluid-fluid interface forms a curve-shaped meniscus with the contact angle as large as 168° (Fig. 4a). To function as a tunable liquid prism, we applied various ac biases to the left and right sidewalls, while grounding the base substrate, to control the apex angle of the prism. The left sidewall was applied with 19V$_{ac}$ and the right with 48 V$_{ac}$ at 40Hz. Thus the interface orientation was controlled with an apex angle of φ = 22° (Fig. 4b). Figure 4(c) presents a photograph of the interface with φ =
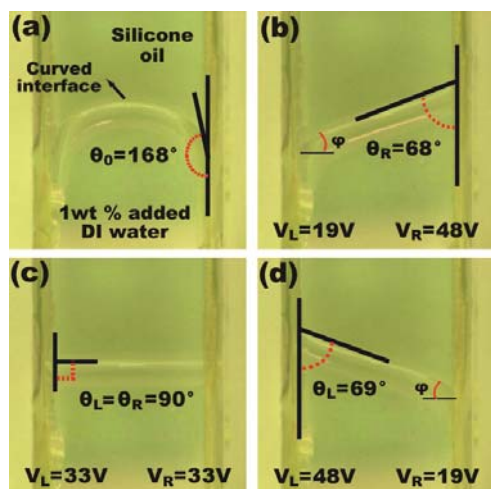
Figure 4. Photographs of an electrowetting-driven liquid prism modulation. (a) Before applying ac bias voltage, the contact angle of water is 168° and the curve-shaped interface is formed. (b) $19V_{ac}$ and $48 V_{ac}$ are applied to the left and right sidewalls at 40Hz. (c) The equal voltage of 33 V_{ac} are applied and the interface is created with an apex angle of 0°. (d) When $48 V_{ac}$ and $19 V_{ac}$ were applied to the left and right sidewalls, the interface orientation was reversely controlled with an apex angle of $\varphi = -21°$.

0°, which was achieved by applying $33V_{ac}$ on the both left and right sidewalls. When $48 V_{ac}$ and $19 V_{ac}$ were applied to the left and right sidewalls, the interface was reversely controlled with an apex angle of $\varphi = -21°$ (Fig. 4d).

6 CONCLUSION

Large portion of the installation cost in a CPV plant is associated with solar tracking systems, because they require complex, bulky, and heavy mechanical tracking components. These issues make CPV difficult to be used for a residential rooftop application. In this paper, we report a low-cost, non-mechanical solar tracking system for a CPV rooftop application. A proposed system consists of an array of tunable liquid prisms that are controlled by an electrowetting effect and enable to track incident sunlight without mechanical moving parts. By eliminating such complex and heavy mechanical solar tracking components, total cost and power consumption of the CPV system are significantly reduced.

Optical analysis has been conducted to predict the prism performance and develop solar control algorithm. A solar tacking capability of the prism is greatly enhanced by increasing the refractive index of the liquid located in the lower side. The dual prism composed of two stacked single prisms can achieve wide tracking range up to ±70°. We have successfully demonstrated elecrtowetting-driven liquid prism modulation using water and silicone oil. The proposed electrowetting-driven solar tracking (EST) system

would be an alternative solution that enables high-efficiency concentrated solar power system on a rooftop.

REFERENCES

[1] S. A, J. Meier, A. Buechel, U. Kroll, J. Steinhauser, F. Meillaud, H. Schade, and D. Domine, "Towards very low-cost mass production of thin-film silicon photovoltaic (PV) solar modules on glass," *Thin Solid Films,* vol. 502, pp. 292-299, 2006.

[2] N. S. Lewis, "Toward Cost-Effective Solar Energy Use," *Science,* vol. 315, pp. 798-801, 2007.

[3] S. Kurtz, "Opportunities and Challenges for Development of a Mature Concentrating Photovoltaic Power Industry," *Technical Report, NREL/TP-520-43208* 2008.

[4] S.-Y. Park, M. A. Teitell, and E. P. Y. Chiou, "Single-sided continuous optoelectrowetting (SCOEW) for droplet manipulation with light patterns," *Lab on a Chip,* vol. 10, pp. 1655-1661, 2010.

[5] M. Abdelgawad, P. Park, and A. R. Wheeler, "Optimization of device geometry in single-plate digital microfluidics," *Journal of Applied Physics,* vol. 105, p. 094506, 2009.

[6] J. Cheng and C.-L. Chen, "Active thermal management of on-chip hot spots using EWOD-driven droplet microfluidics," *Experiments in Fluids,* vol. 49, pp. 1349-1357, 2010.

[7] P. Y. Paik, V. K. Pamula, and K. Chakrabarty, "Adaptive Cooling of Integrated Circuits Using Digital Microfluidics," *IEEE Transactions on Very Large Scale Intergration (VLSI) Systems,* vol. 16, pp. 432-443, 2008.

[8] E. Baird and K. Mohseni, "Digitized Heat Transfer: A New Paradigm for Thermal Management of Compact Micro Systems," *IEEE Transactions on Components and Packaging Technologies,* vol. 31, pp. 143-151, 2008.

[9] R. A. Hayes and B. J. Feenstra, "Video-speed electronic paper based on electrowetting," *Nature,* vol. 425 pp. 383–385 2003.

[10] N. Chronis, G. Liu, K.-H. Jeong, and L. Lee, "Tunable liquid-filled microlens array integrated with microfluidic network," vol. 11, pp. 2370-2378, 2003.

[11] M. Vallet, B. Berge, and L. Vovelle, "Electrowetting of water and aqueous solutions on poly(ethylene terephthalate) insulating films " *Polymer,* vol. 37, pp. 2465-2470 1996.